

An Implicit Unsteady Finite Volume Formulation for Natural Convection in a Square Cavity

Edoardo Bucchignani¹

Abstract: This article describes an implicit method for the solution of time dependent Navier-Stokes equations written in terms of vorticity and velocity. The field equations are discretized using a finite volume technique over quadrilateral meshes.

The numerical code has been applied to the classical window cavity test, employing a fine stretched non-uniform grid, in order to provide an accurate steady solution for a high value of the Rayleigh number (10^8). It has also been performed a simulation for a value of Rayleigh larger than the critical value, in order to show the capabilities of the proposed method to properly simulate the unsteady regime.

1 Introduction

In the last decade, implicit methods became more popular in research and industry because of their stability and robustness when used in everyday applications. Especially in the field of computational fluid dynamics, a large effort has been done in order to develop robust and efficient flow solvers based on fully implicit approaches. The benefits of such methods are well known: a greater robustness, allowing the capability of solving problems that cannot be handled with explicit schemes; moreover, they allow the possibility of using larger time steps, reducing the global cpu-time. Promising results have been obtained and very stiff cases have been solved. However, the practical use of implicit based codes has been significantly limited, because they require a large amount of computational resources when fine computational grids are adopted. In fact, implicit schemes request the solution of large sparse linear systems of equations, whose sizes grows linearly with the number of grid-points, while the cpu-time grows with the cube of the number of unknowns. It is clear that with the computational resources available in the '90, it was impossible to deal with systems characterized by millions of unknowns. In several sectors such as the aerospace, where very fine computational meshes are needed, the use of implicit methods was prohibitive and for this reason they have

¹ Centro Italiano Ricerche Aerospaziali, Via Maiorise, 81043 Capua (CE) - Italy

been neglected. Only in the last three years, with the fast increase of the computational power even on a notebook, there has been a renewed interest for implicit schemes as it is now possible to take into account such methods for practical applications, on very fine grids.

Stella and Bucchignani (1996) introduced a true transient vorticity-velocity formulation for incompressible two dimensional flows, based on a finite difference approximation of the governing equations and using a fully implicit approach for the time integration. The linear systems arising from discretization were solved by using a preconditioned Bi-CGSTAB algorithm. The code was used to obtain steady solutions of the window cavity (test case defined by de Vahl Davis (1983) at values of the Rayleigh (Ra) number in the range $10^4 - 10^8$. Even if the solutions obtained were sufficiently accurate, it was not possible to perform numerical simulations on meshes with more than $257 \cdot 257$ points.

Successively, in 1999 the proposed methodology was extended to three dimensional flows (see Stella and Bucchignani, 1999, Bucchignani and Stella, 1999) and successfully used for solving problems of natural convection in limited domains (Bucchignani and Mansutti, 2000, Bucchignani, 2004) showing the effectiveness of the vorticity-velocity formulation also for three dimensional cases.

However, the finite difference approach allowed to use only regular cartesian meshes, while it is well known that, in order to obtain an accurate resolution of the boundary layers, stretched variable grids must be employed. For this reason, with the aim of better exploiting the computational resources available nowadays, in this work it has been developed a numerical code based on a finite volume discretization of the governing equations, associated with a fully implicit approach for the time integration. In this way, also very fine non uniform meshes can be adopted. Furthermore, a procedure that ensures good coupling between the equations has been adopted, in order to guarantee the mass conservation together with a second order accuracy in time. It is worth to point out that this methodology allows the simulation of more complicated geometries (not only rectangular domains) or domain with a time dependent shape.

This numerical code has been applied to the classical window cavity, in order to provide more accurate results than those provided in 1996. In spite of its apparent simplicity, it represents a serious test case from a computational point of view, especially at high values of the Rayleigh number (10^8 and larger values). It is not simple to find an accurate solution, as evidenced by the significant discrepancy of the existing results. In fact, this problem has been investigated by several authors, with different numerical models. In 1983, de Vahl Davis (1983) provided a benchmark solution for this problem, assuming the Prandtl number (Pr) equal to 0.71, for values of Ra limited to 10^6 . Successively, Le Queré (1991) provided

accurate results also for higher values of Ra (10^7 and 10^8). In 1994, Ravi, Henkes and Hoogendoorn (1994) performed an analysis of the flow structure evolution in the corner region of the cavity, as the value of Ra is increased. Numerical results were provided also by Mayne, Usmani and Crapper (2000), who employed an h -adaptive finite element method, founding a good agreement with Le Queré. Wan, Patnaik and Wei (2001) introduced a quasi-wavelet-based discrete singular convolution (DSC) to solve the window cavity, presenting benchmark quality data for the range $10^3 \leq Ra \leq 10^8$. Their results match quite good with previous ones, even if DSC seems to fail to accurately simulate the velocity field in the boundary layers at high Ra . In a recent paper, Dixit and Babu (2006) used a thermal lattice Boltzmann method to simulate natural convection in a square cavity for high Ra , as a novel alternative to traditional numerical methods. Their results show good agreement with reference ones at small-medium values of Ra , but for larger values the discrepancy is not negligible, also due to the unsteadiness of the flow that is not taken into account by their model. Finally, Gelfgat (2006) applied the global Galerkin or weighted residuals method to the incompressible Navier-Stokes equations, providing good quality results.

It is evident that the window cavity still represents an useful test case to evaluate the power and correctness of numerical codes. The difficulties are increased by the transition to the unsteady periodic regime that, from the numerical findings of Le Queré and Behnia (1998), should appear at about $Ra = 1.82 \cdot 10^8$. The benefits of implicit time integration procedures are not so obvious for solving unsteady flows, because the CFL number must be anyhow of the order of unity, otherwise there could be a lack of accuracy in the transient histories if the time step is too large. However, in the opinion of the author, the use of implicit methods is always strongly recommended, because at these large values of Ra , explicit or ADI solver based codes need very small CFL (order of 0.001 or smaller) and in some cases it has been experienced that they do not allow the possibility to simulate these cases, whatever was the CFL chosen.

The main aims of this paper are:

- to describe the implicit numerical model adopted, and particularly the spatial discretization of the incompressible Navier-Stokes equations in vorticity-velocity formulation;
- to show the capabilities of the code to accurately simulate domains with very fine meshes with second order accuracy in reasonably limited cpu-time even on a notebook;
- to provide a more accurate steady solution of the window cavity at $Ra = 10^8$ with respect to the one obtained in the previous work, Stella and Bucchignani (1996);
- to provide a description of an unsteady solution, for a value of the Rayleigh num-

ber ($Ra = 2 \cdot 10^8$) larger than the critical value, with analysis of the transient histories and flow configurations.

The paper is organized as follows: in Sec. 2 the mathematical model is briefly recalled; in Sec. 3 the numerical method is widely explained and in Sec. 4, after a short description of the problem, results are presented, both for the steady and for the unsteady case.

2 Mathematical model

2.1 Governing equations

The mathematical model is widely explained in Stella and Buchignani (1996); however, it is briefly recalled here. The vorticity-velocity form of the non-dimensional equations governing two-dimensional natural convection for a Newtonian fluid, assuming the Boussinesq approximation to be valid, is (Guj and Stella, 1993):

$$\frac{1}{Pr} \frac{\partial \boldsymbol{\omega}}{\partial t} + \frac{1}{Pr} \nabla \cdot (\mathbf{u} \boldsymbol{\omega}) = \nabla^2 \boldsymbol{\omega} - Ra \nabla \times \left(\theta \frac{\mathbf{g}}{|\mathbf{g}|} \right) \quad (1)$$

$$\nabla^2 \mathbf{u} = -\nabla \times \boldsymbol{\omega} \quad (2)$$

$$\frac{\partial \theta}{\partial t} + (\mathbf{u} \cdot \nabla) \theta = \nabla^2 \theta \quad (3)$$

where $\boldsymbol{\omega}$ is the vorticity vector, $\mathbf{u}(u, v, 0)$ is the velocity vector and θ is the temperature. The non-dimensional parameters Ra and Pr are defined as:

$$Ra = \frac{g\beta\Delta TL^3}{\kappa\nu} \quad Pr = \frac{\nu}{\kappa}$$

in which g is the gravitational acceleration, β is the coefficient of thermal expansion, L is the size of the box, ΔT the temperature difference between hot and cold walls, κ the thermal diffusivity and ν is the kinematic viscosity. The non-dimensional scheme is based on a reference velocity \mathbf{u}^* defined as κ/L and a reference time t^* defined as L^2/κ .

The vorticity $\boldsymbol{\omega} = (0, 0, \omega)$ is defined as usual:

$$\boldsymbol{\omega} = \nabla \times \mathbf{u} \quad (4)$$

where, because the flow is two-dimensional, only the third component of $\boldsymbol{\omega}$ is obviously non-zero.

Heat flux, from hot to cold wall, has been evaluated using the proper definition of the mean Nusselt number on a vertical section:

$$Nu = \frac{1}{S} \int_S (\theta \mathbf{u} - \nabla \theta) \cdot \mathbf{n} dS \quad (5)$$

2.2 Boundary conditions

The above formulation allows a very simple form of the boundary conditions:

- the boundary conditions associated to eq. (1) are obtained by the vorticity definition written on the boundary.
- Dirichlet boundary conditions are associated to the elliptic velocity equation (2). In particular null velocity field is assigned at the solid walls.
- the boundary conditions for the energy equation are easily derived from the definitions and are of Dirichlet or Neumann type in those portions of the boundary where respectively the value of temperature or its normal derivative are known.

$$\begin{aligned} \theta &= T_h & \{ x = 0 \\ \theta &= T_c & \{ x = L \\ \frac{\partial \theta}{\partial n} &= 0 & \{ y = 0, y = H \end{aligned}$$

3 Numerical method

As already explained in the Introduction, the methodology proposed in this paper is an extension of an existing one introduced by Stella and Bucchignani (1996). In that work, the governing equations were discretized using a finite difference technique on a uniform cartesian grid. The time integration was performed by means of a fully implicit approach and solving the linear system arising from discretization using an iterative method belonging to the Krylov subspace class. It was opinion of the authors that proposed methodology represented a useful compromise between numerical efficiency and robustness. It is worth noting that it allows easy and straight-forward applications on parallel computers, subdividing the coefficient matrix in horizontal bands, each of them is assigned to a processor, allowing to obtain the same transient history as on a uniprocessor machine, with interesting values of speed-up.

Its main lack was of course the scarce flexibility in applications, due to the discretization performed on cartesian grids, that limits the use only to regular domains. For this reason, in order to overcome this problem, in this work the governing equations have been discretized using a finite volume approximation on a non uniform mesh made up of quadrilateral elements, following the approach described in Fletcher (1991). Each equation is integrated over an appropriate control surface, as proposed by Labonia, Stella, Leonardi and Guj (1997). Staggering of

the variable locations has been chosen in order to obtain the maximum accuracy of the discretized terms.

The time derivative and the convective term in the vorticity equation are discretized using the control surface shown in Fig. 1. Due to the staggering of the variables, none of the unknowns is positioned at the points labelled with e , w , n , s , so they are evaluated by averaging the values of the variables in the computational nodes rounding the mentioned points.

In a similar manner, the time derivative and the convective term of the energy equations have been discretized using the control surface shown in Fig. 2.

The Laplacian term in the vorticity equation has been discretized by means of the formula described, for example, in Labonia, Stella, Leonardi and Guj (1997), considering the same control surface of Fig. 1. The Laplacian terms contained in the energy equation and velocity equations have been discretized in the same way, but assuming different control surfaces. The buoyancy term in the vorticity equation and the spatial derivatives of ω in the velocity equations are discretized without particular difficulties.

The time integration of non-linear systems has two important aspects: time discretization and treatment of the non-linear terms. For what concerns the first topic, a three point second order backward difference is employed in this work, which is commonly used. Implicit methods differ one another by the way in which non-linear terms are treated. A simple solution consists in decoupling the equations (as in the SIMPLEC algorithm, Barakos and Mitsoulis, 1994); however, a procedure that ensures good coupling between the equations has been preferred (Lowrie, 2004), in order to guarantee mass conservation. In fact, since the continuity equation is not explicitly imposed, mass conservation and definition of vorticity could be violated, if good coupling between the full set of the equations is not ensured. The procedure adopted is the following: let us consider a non-linear term, for example a convective term in the vorticity equation (i.e. $u\omega$). If u^0 and ω^0 are the known values (at the previous time step), and Δu and $\Delta\omega$ are the variations (to be calculated), the non-linear term can be written as:

$$u\omega = (u^0 + \Delta u)(\omega^0 + \Delta\omega) = u^0\omega^0 + u^0\Delta\omega + \omega^0\Delta u + \Delta u\Delta\omega \quad (6)$$

the last term can reasonably be neglected, obtaining the searched linearization. This procedure leads to a large sparse linear system of equations $\mathbf{R}x = b$ to be solved at each time step. The Bi-CGSTAB algorithm (Van der Vorst, 1992) has been adopted, because of its numerical stability and speed of convergence. Bi-CGSTAB is an iterative method belonging to the Krylov subspace class. Although, from a theoretical point of view, iterative methods can be used without preconditioning the linear systems of equations, the use of a preconditioning technique is, in many

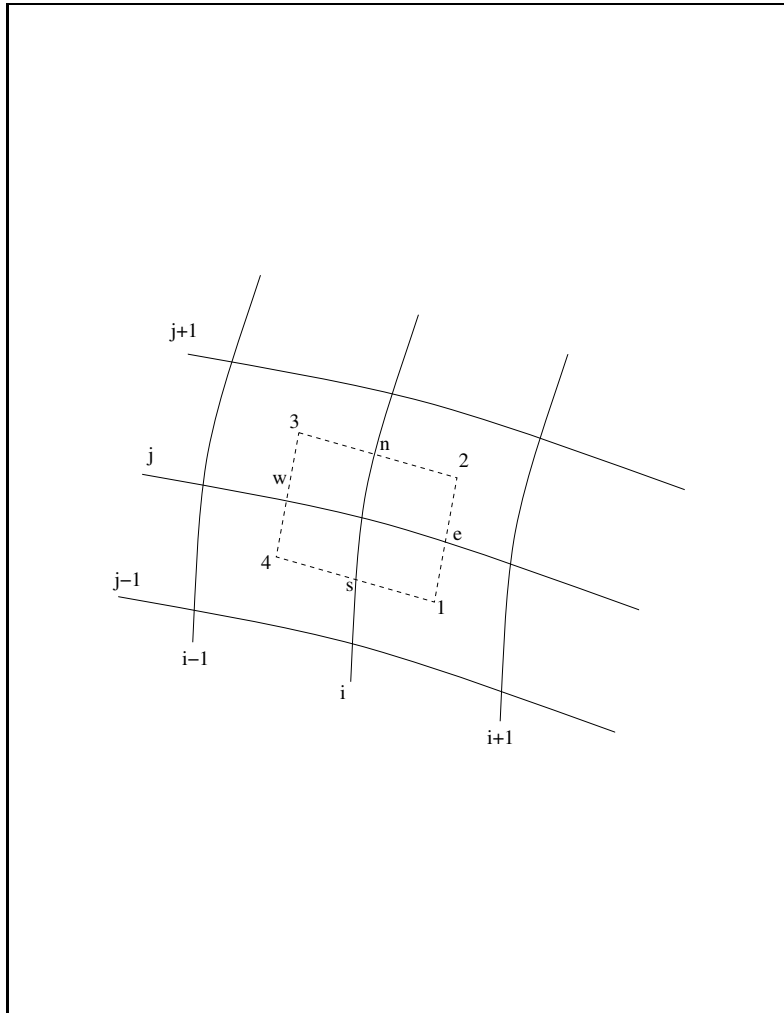


Figure 1: Control surface for the discretization of the convective term in vorticity equation.

practical applications, essential to fulfil the convergence and stability requirements of the iterative procedure itself. In this work a ILU factorization has been adopted as preconditioner.

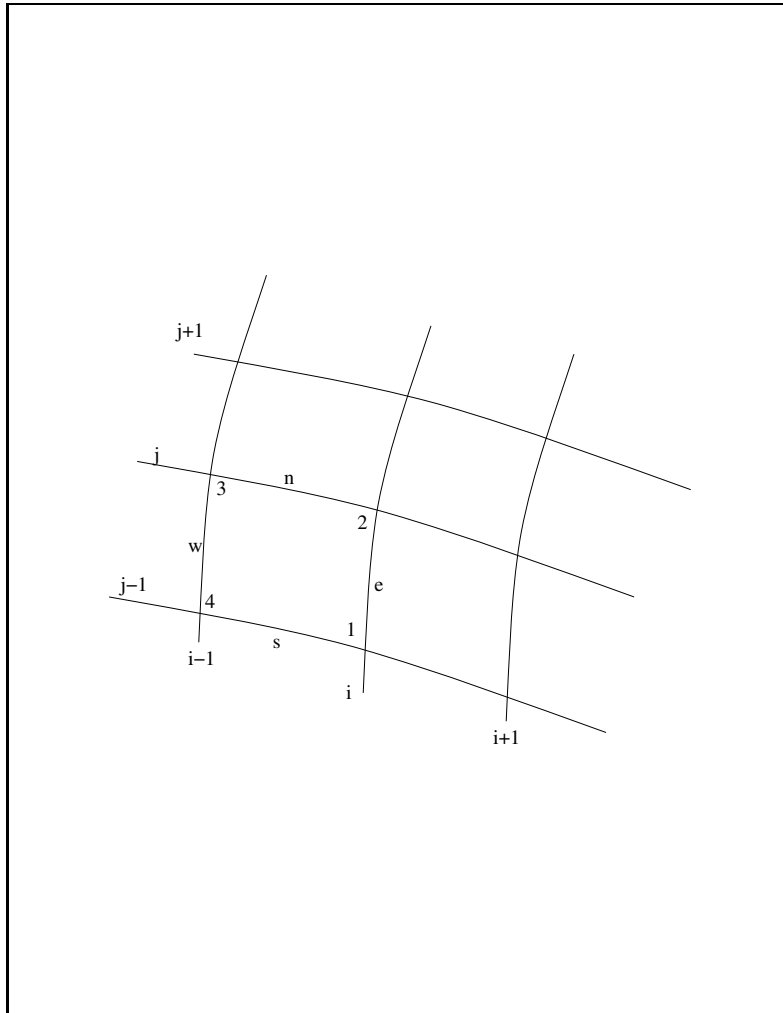


Figure 2: Control surface for the discretization of the convective term in energy equation.

4 Results

4.1 Description of the problem

The problem under consideration is depicted in Fig. 3.

The flow domain is the interior of a 2D square cavity ($L = H$). The horizontal walls are assumed to be perfectly adiabatic, while the vertical walls are kept isothermal with the left wall at high temperature T_h and the right wall at low temperature T_c .

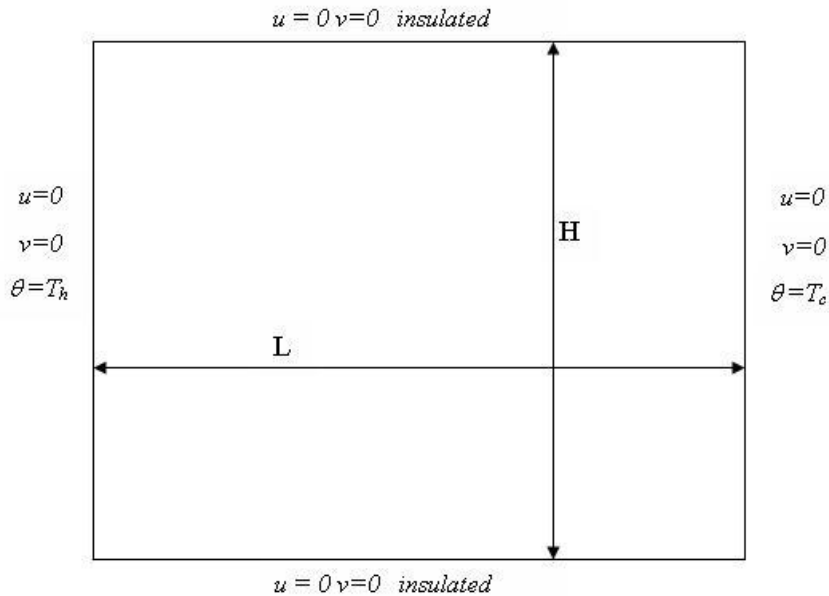


Figure 3: The square cavity with boundary conditions.

The cavity is filled with air, and all the properties are calculated at a reference temperature of 273 K. In such conditions, the Prandtl number is equal to 0.71 and is kept constant. Owing to heat transfer, density changes result in a recirculating flow.

4.2 Steady solution

The first simulation has been performed at $Ra = 10^8$, which is the larger values usually adopted by researchers to compare steady solutions of the window cavity. The results obtained by the author (Stella and Bucchignani, 1996) using a finite difference code were affected by an error generally three to four times higher with respect to those obtained at lower values of Ra . This indicates greater difficulty in the resolution of thermal and kinematic boundary layers at this high value of Ra with a uniform grid. As suggested by Barakos and Mitsoulis (1994), the use of non-uniform meshes is recommended, since the influence of the steep gradients near solid walls dominates at high Ra : the node density is higher near the walls of the cavity. An example of non-uniform grid is shown in Fig. 4.

As usual, it has been assumed that $L = H = 1$, $T_h = 1$, $T_c = 0$ (non dimensional values). All the numerical simulations have been performed on a PC - Pentium IV

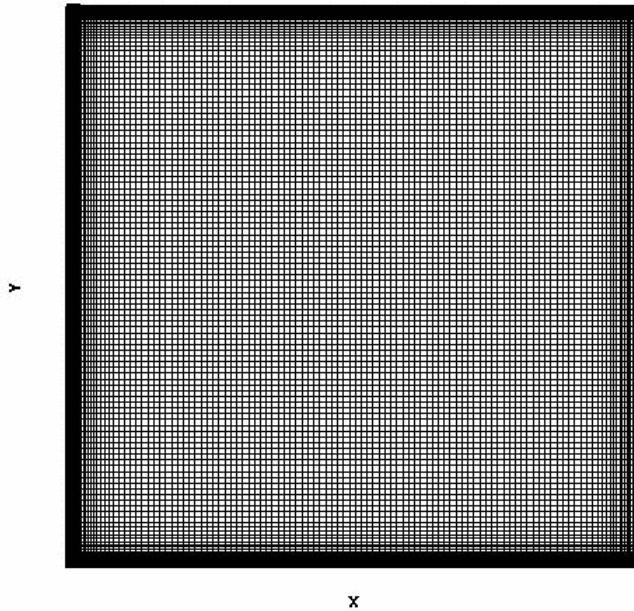


Figure 4: The computational grid with $129 \cdot 129$ points.

3 GHz with 1 GB of memory.

A mesh sensitivity analysis has been performed, considering three different grids: $129 \cdot 129$, $257 \cdot 257$ and $513 \cdot 513$. The maximum and minimum values of the cell size for each mesh are reported in Tab. 1, together with the maximum allowable value of the time step and with the cpu-time required to perform a single iteration. In all the cases the CFL order of magnitude is unity. The simulation on the grid $129 \cdot 129$ has performed starting from rest. The simulation on the grid $257 \cdot 257$ has been performed starting from a flow field obtained by appropriately interpolating the steady solution on the grid $129 \cdot 129$. And in the same way, the computation on the grid $513 \cdot 513$ has been started from a flow field obtained by appropriately interpolating the steady solution on the grid $257 \cdot 257$. For this reason, the global cpu-time required to reach the steady state does not grow quickly with the size of the problem, being on the three grids respectively equal to 40, 250 and 530 hours.

The following quantities have been selected for the comparison:

$|\psi|_{max}$ the maximum value of the stream function ψ ;

Table 1: Maximum and minimum values of the cell size, maximum time step, cpu-time x iteration for each mesh.

mesh	max Δx	min Δx	Δt	cpu x it.
129 · 129	10^{-2}	10^{-3}	10^{-6}	3.2 sec
257 · 257	$5 \cdot 10^{-3}$	$5 \cdot 10^{-4}$	10^{-7}	16 sec
513 · 513	$2.5 \cdot 10^{-3}$	$2.5 \cdot 10^{-4}$	$2 \cdot 10^{-8}$	69 sec

$|\psi|_{mid}$ the value of the stream function ψ in the centre of the cavity;

u_{max} the maximum value of the horizontal velocity distribution at the mid width ($x = 0.5$) (together with its location);

v_{max} the maximum value of the vertical velocity distribution at the mid height ($y = 0.5$) (together with its location);

U_{max} the maximum value of the horizontal velocity component on the whole domain;

V_{max} the maximum value of the vertical velocity component on the whole domain;

$Nu_{1/2}$ the average Nusselt number on the vertical mid-plane of the cavity;

\overline{Nu} the average Nusselt number throughout the cavity;

Nu_0 the average Nusselt number on the vertical left wall;

Nu_L the average Nusselt number on the vertical right wall;

that are the same proposed by de Vahl Davis (1983) with the addition of the maximum values of the velocity components on the whole domain, proposed by Wan, Patnaik and Wei (2001).

Tab. 2 reports the values of these quantities obtained on each grid. The analysis of the table confirms that the numerical model is “nearly” second order accurate in space. Besides, being a difference lesser than 1 % between the values of each velocity component obtained on the different grids, the results are “mesh - independent”. The percentage error for Nu is slightly higher: this difficulty in numerical convergence of Nu has been already observed (Stella, Guj and Leonardi, 1993) and is related to the calculation of Nu which is a derived quantity in the vorticity-velocity formulation.

Table 2: Steady solution: mesh sensitivity analysis.

	129 · 129	257 · 257	513 · 513
ψ_{mid}	52.40	52.43	52.44
ψ_{max}	53.84	53.89	53.90
U_{max}	1127.6	1125.9	1125.4
V_{max}	2227.6	2233.5	2235.1
u_{max}	315.4	320.4	321.7
v_{max}	2224.4	2224.3	2224.3
$Nu_{1/2}$	32.72	30.78	30.15
\overline{Nu}	29.31	28.78	28.42
Nu_0	29.22	28.80	28.57
Nu_L	1.94	1.92	1.92

Streamlines contour plots and isothermal lines are shown in Fig. 5 and 6. An analysis of the pictures shows that, as already found in previous works, the temperature and velocity fields are skew symmetric with respect to the centre of the computational domains. While for smaller values of Ra the heat transfer is mainly due to conduction, increasing Ra causes a change of heat transfer mechanism, in fact convection tends to become dominant: the isothermal lines are vertical everywhere, being horizontal only in the proximity of vertical walls (very thin thermal boundary layer).

As already described in the Introduction, the window cavity problem has been investigated by several authors, with different numerical techniques, so a large amount of data is available for comparison. Tab. 3 reports some of the quantities found in literature, together with the present results.

The analysis of Tab. 3 allows the following considerations. First, it is evident that the use of non-uniform meshes significantly increases the quality of the solution. In fact, assuming the data of Le Queré (1991) as reference, the error that affects the present results obtained on the grid 257 · 257 is lower than the error related to the solution obtained by the author on a uniform grid (Stella and Bucchignani, 1996) with the same number of points. The vertical velocity distribution has a direct relation to the size of the boundary layers near the hot and cold walls: the non-uniform grid 513 · 513 allows an optimal resolution of the vertical boundary layers, as stated by the excellent agreement of v_{max} , concerning both the value (error 0.1 %) and its location. The same good agreement is registered for u_{max} and for the values of ψ , even if ψ is a derived variable in the present formulation. Fig. 7 shows

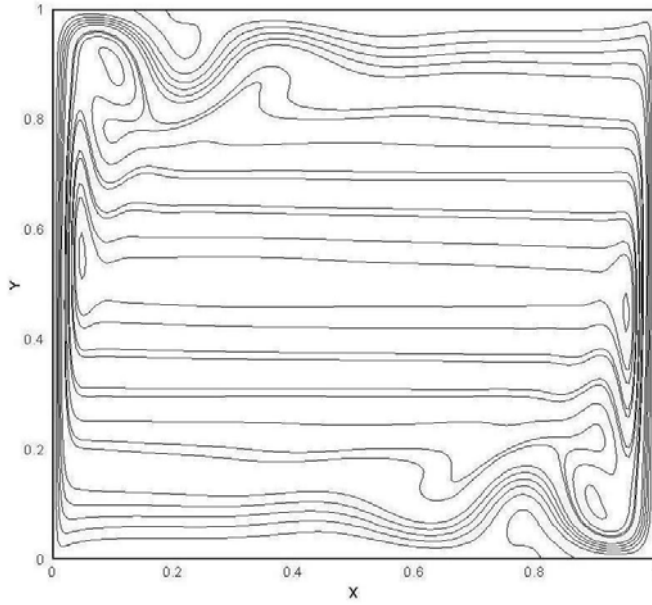


Figure 5: Streamlines at $Ra = 10^8$.

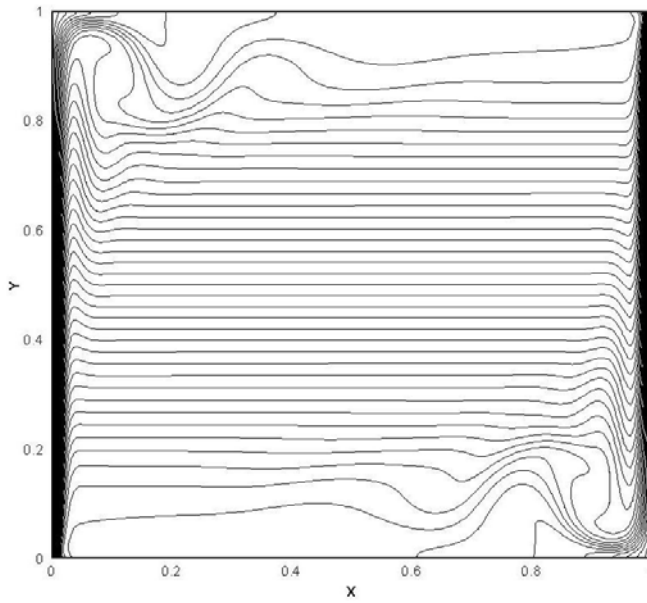


Figure 6: Isothermal lines at $Ra = 10^8$.

Table 3: Steady solution: comparison of the current solution on the grids $257 \cdot 257$ and $513 \cdot 513$ with available data. (1) Stella and Bucchignani (1996), (2) Le Queré (1991), (3) Mayne and Usmani (2000), (4) Wan, Patnaik and Wei (2001), (5) Dixit and Babu (2006), (6) Gelfgat (2006)

	257 · 257	513 · 513	(1)	(2)
Ψ_{mid}	52.43	52.44	52.97	52.32
Ψ_{max}	53.89	53.90	54.44	53.85
u_{max}	320.4	321.7	326.48	321.90
x	0.914	0.925	0.931	0.928
v_{max}	2224.3	2224.3	2200.9	2222.0
y	0.015	0.015	0.017	0.012
U_{max}	1125.9	1125.4	-	-
V_{max}	2233.5	2235.1	-	-
$Nu_{1/2}$	30.78	30.15	30.75	30.22
Nu	28.78	28.42	30.75	-
Nu_0	28.80	28.57	30.75	30.22
Nu_L	1.92	1.92	1.90	1.92
	(3)	(4)	(5)	(6)
Ψ_{mid}	-	-	-	52.32
Ψ_{max}	-	-	-	53.84
u_{max}	283.6	295.7	373.8	321.86
x	0.94	0.940	0.933	0.927
v_{max}	2223.4	2290.1	2256.5	2222.28
y	0.013	0.013	0.0112	0.012
U_{max}	-	1006.3	-	-
V_{max}	-	2293.6	-	-
$Nu_{1/2}$	-	-	-	-
Nu	-	23.67	30.15	-
Nu_0	29.62	-	-	30.22
Nu_L	-	1.43	-	-

the temperature profile at $y = 0.5$ and Fig. 8 shows a close-up view of the boundary layer near the left wall.

A scarce agreement with the results of Wan, Patnaik and Wei (2001) is observed, being the discrepancy included in the range 3 - 10 %, with larger errors for the horizontal velocity components. They used a DSC approach that, in spite of several advantages, seems not suitable for high Ra fields, because it is not able to accurately simulate the velocity distribution in the boundary layer. This is also confirmed by the large error on U_{max} , which is localized at a point close to the top left corner of the cavity. For what concerns the solution of Dixit and Babu (2006), they provide a value of u_{max} that is very different from the one of other authors. The possible reason is that their solution is not really "mesh - independent" because, in spite of a fine grid adopted ($512 \cdot 512$), they report a non negligible difference (4 %) between the solutions obtained on consecutive grids. Finally, a quantitative comparison with the results of Ravi, Henkes and Hoogendoorn (1994) is not possible, because they do not provided the values used in Tab. 3, however the streamlines contour plot of Fig. 5 looks very close to their analogous plot.

4.3 Unsteady solution

In contrast to steady solutions, only a few numerical simulations of unsteady flows have been performed in cavities heated from a side. From the stability linear analysis (P. Bergé, Pomeau and Vidal, 1984) it is detected that, when a system undergoes a supercritical Hopf bifurcation (as in the present case), a complex pair of eigenvalues of the Jacobian crosses the imaginary axis, giving rise to a perturbation that causes unsteadiness and could break the skew symmetry of the field.

The critical value of Ra for the transition to the unsteady periodic regime was evaluated, with a reasonable degree of certainty, by Le Queré and Behnia (1998) and is equal to $1.82 \pm 0.01 \cdot 10^8$. In order to show the capabilities of the proposed method to properly simulate the unsteady regime, a simulation was performed at $Ra = 2 \cdot 10^8$, using the same grid ($257 \cdot 257$) already described in the previous subsection, and assuming a time step $\Delta t = 10^{-7}$.

In Tab. 4 the oscillation frequency and the maximum value of the vorticity at the point C (see below) obtained using different time steps are shown, in order to evaluate the accuracy of the numerical scheme with respect to time derivative. The results obtained show that method is second order accurate with regards to time discretization, and that $\Delta t = 10^{-7}$ (the CFL order of magnitude is unity) provides results sufficiently accurate for our purposes.

It is well known that in the steady regime the solution does not depend on the initial conditions, but this is not true when the solution becomes time dependent, so

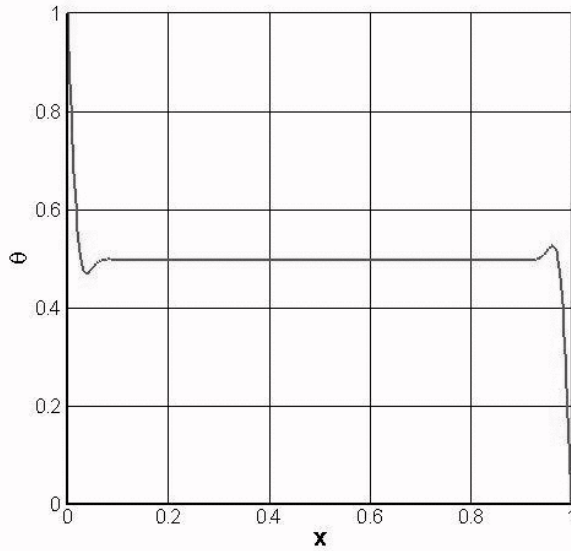


Figure 7: Temperature profile at $Ra = 10^8$, at $y = 0.5$: entire cavity.

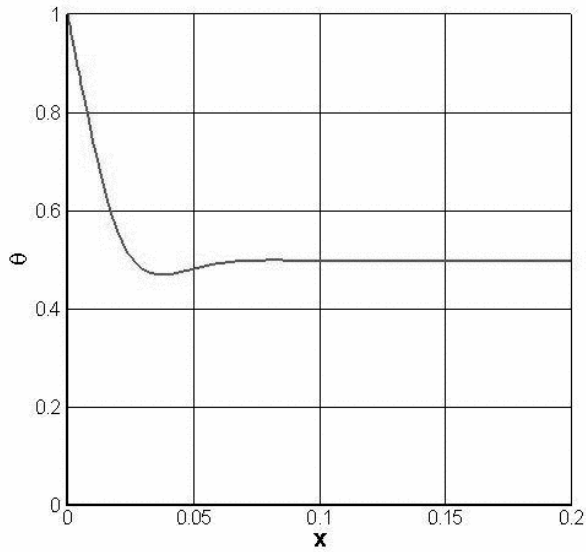


Figure 8: Temperature profile at $Ra = 10^8$, at $y = 0.5$: close up view near the left wall.

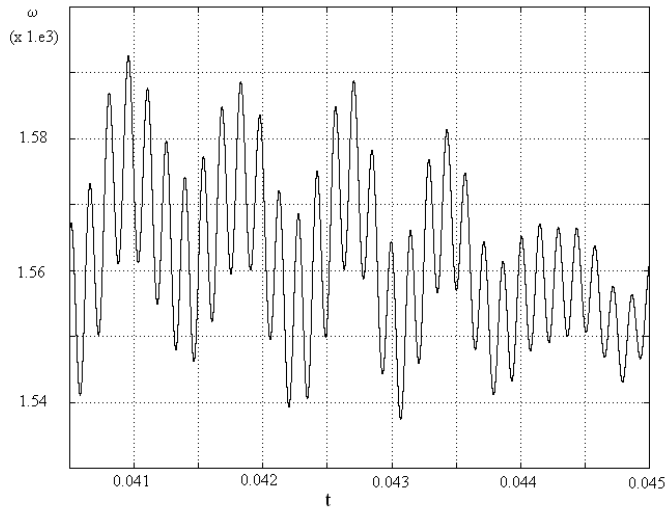


Figure 9: Time history of ω at $Ra = 2 \cdot 10^8$, at the point $C(0.007, 0.81)$.

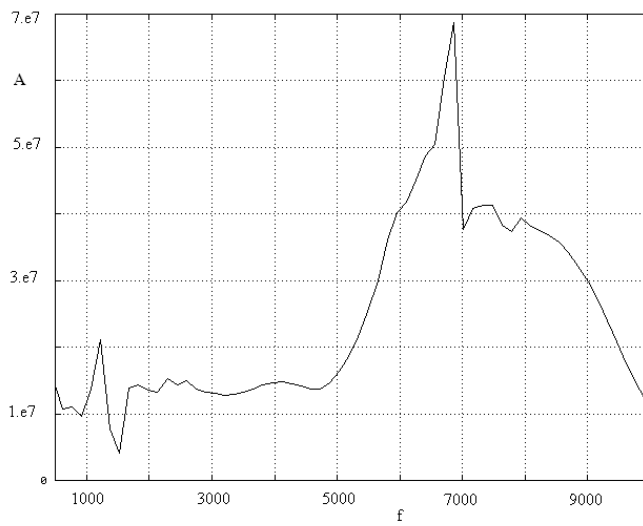


Figure 10: Frequency analysis of the time history of ω at $Ra = 2 \cdot 10^8$, at the point $C(0.007, 0.81)$.

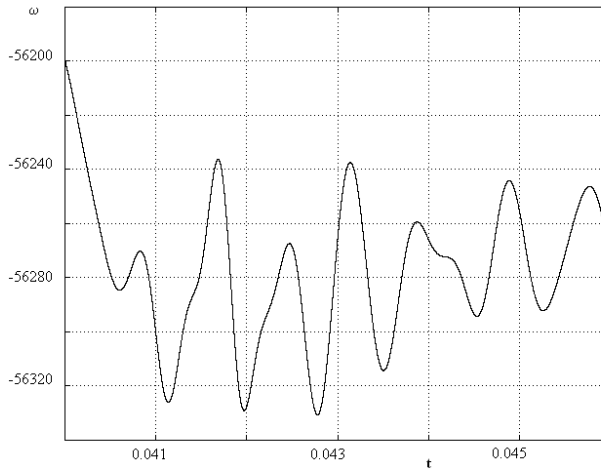


Figure 11: Time history of ω at $Ra = 2 \cdot 10^8$, at the point $A(0.007, 0.007)$.

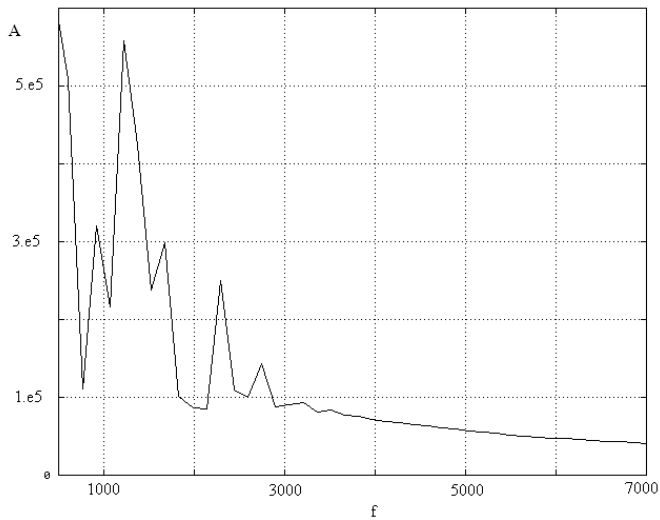


Figure 12: Frequency analysis of the time history of ω at $Ra = 2 \cdot 10^8$, at the point $A(0.007, 0.007)$.

Table 4: Unsteady solution: time step sensitivity analysis.

	$\Delta t = 2 \cdot 10^{-7}$	$\Delta t = 10^{-7}$	$\Delta t = 5 \cdot 10^{-8}$
f	6873.86	6866.50	6864.61
ω_{max}	159324.7	159236.6	159214.3

in this case they must be clearly specified. In this work, the steady field obtained at $Ra = 10^8$ has been used as initial condition. The time histories of the flow variables have been monitored in five distinct points: $A(0.007, 0.007)$, $B(0.81, 0.007)$, $C(0.007, 0.81)$, $D(0.81, 0.81)$ and $E(0.15, 0.88)$. The first four points are located in the proximities of the four corners, while the last one is the point that was selected by Le Queré and Behnia (1998). The analysis of the time histories shows that the flow is quasi-periodic with two incommensurate frequencies. This regime is characterized by a couple of fundamental frequencies that could be different from a point to another. Fig. 9 shows the time history of the vorticity at the point C and Fig. 10 shows the FFT performed on this signal (65536 samples): it is characterized by a main frequency $f_1 = 6866.5$ (non-dimensional units), which is modulated by a lower frequency $f_2 = 1220.7$. The same behaviour is observed also at the point E . Instead, the vorticity signal at the point A differs (Fig. 11 and 12), because in this case the main frequency is f_2 , modulated by a lower one $f_3 = 915.5$. Besides, at the point B the couple of frequencies is $f_4 = 610.35$ and $f_5 = 1068.11$, while at the point D is f_2 and f_5 . It is worth noting that, at each point, the behaviour of the other flow variables (u , v , θ) is analogous to that of ω , with the same frequencies of oscillations.

Fig. 13 shows the streamlines at $Ra = 2 \cdot 10^8$ for four different time steps: t_1 (beginning of a period), $t_2 = t_1 + Tp/4$, $t_3 = t_1 + 2 \cdot Tp/4$, $t_4 = t_1 + 3 \cdot Tp/4$, where $Tp = 1/f_2$. This picture shows that the flow configuration continues to be skew symmetric at each time step, highlighting that the perturbations (numerical and physical) at this value of Ra are not sufficient to break the symmetry. This should happen at larger values of Ra , but this analysis is beyond the purpose of the present paper.

A comparison with the results of Le Queré and Behnia (1998) is not immediate, because they used a different non-dimensional scheme. However, starting from the same initial conditions, they also found a skew symmetric configuration; concerning the time regime, they found at the point E a fundamental period equal to 22.07 non-dimensional units. The period evaluated in the present work is $Tp_1 = 1/f_1 = 1.456 \cdot 10^{-4}$ and making the opportune unit conversions, it cor-

responds to 20.59 non-dimensional units (scheme of Le Queré Behnia). This is of course a good agreement, also taking into account the FFT introduces a further numerical error.

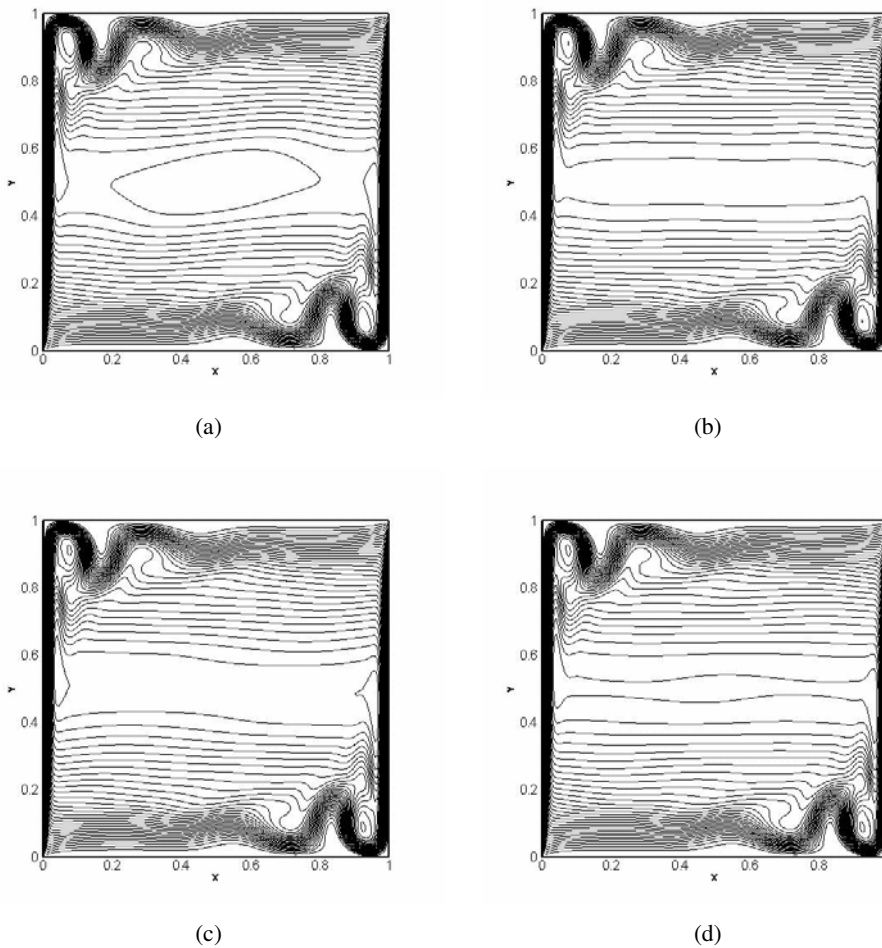


Figure 13: Streamlines at $Ra = 2 \cdot 10^8$ for four different time steps: (a) t_1 (beginning of a period), (b) $t_2 = t_1 + Tp/4$, (c) $t_3 = t_1 + 2 \cdot Tp/4$, (d) $t_4 = t_1 + 3 \cdot Tp/4$.

5 Conclusions

A fully implicit finite volume formulation for the incompressible Navier-Stokes equations has been described. The fast increase of computational power occurred in the last few years has given rise to a renewed interest for the implicit methods, making them appealing for practical everyday applications.

The proposed method allows the possibility of using non-uniform meshes, representing an improvement of the formulation introduced by Stella and Bucchignani (1996).

The method has been applied to the classical window cavity problem at high values of Ra . It has been shown that the code is able to accurately simulate domains with very fine meshes in reasonably limited cpu-time, obtaining an excellent agreement of a steady solution at $Ra = 10^8$ with a reference one.

An unsteady case has also been efficiently simulated, for a value of Ra ($2 \cdot 10^8$) larger than the critical value, with analysis of the transient histories and flow configurations. The regime is quasi periodic with two incommensurate frequencies, while the flow structure changes periodically, but continues to be skew symmetric at each time step.

The present numerical code can also be applied to the simulation of domains with a more complex shape, for example a box with curvilinear walls, or also domains with a time-dependent shape: this occurs in the case of melting problems (Mansutti and Bucchignani, 2005), which could benefit of such kind of methodology, or also domains with a mobile free surface (Bucchignani, Stella and Paglia, 2004). This will be the subject of future work.

References

- Barakos, G.; Mitsoulis, E.; Assimacopoulos, D.** (1994): Natural convection flow in a square cavity revisited: laminar and turbulent models with wall functions, *Int. J. Num. Meth. Fluids*, vol. 18, pp. 695-719.
- Bergé, P.; Pomeau, Y.; Vidal, C.** (1984): *Order within chaos - Towards a deterministic approach to turbulence*, John Wiley & sons.
- Bucchignani, E.; Stella, F.** (1999): Rayleigh - Bénard convection in limited domains: Part 2 - Transition to chaos, *Num. Heat Transfer Part A*, vol. 36, pp. 17-34.
- Bucchignani, E.; Mansutti, D.** (2000): Horizontal thermal convection in a shallow cavity: oscillatory regime and transition to chaos, *Int. J. Numer. Meth. Heat Fluid Flow*, vol. 10, pp. 179-185.
- Bucchignani, E.; Stella, F.; Paglia, F.** (2004): A partition method for the solution of a coupled liquid-structure interaction problem, *Applied Numerical Mathematics*

vol. 51, n.4, pp. 463-475.

Bucchignani, E. (2004): Numerical characterization of hydrothermal waves in a laterally heated shallow layer, *Physics of Fluids*, vol. 16, n. 11, pp. 3839-3849.

de Vahl Davis, G. (1983): Natural Convection of Air in a Square Cavity: a Bench Mark Numerical Solution, *Int. J. Num. Meth. Fluids*, vol. 3, pp. 249-264.

Dixit, H. N.; Babu, V. (2006): Simulation of high Rayleigh number natural convection in a square cavity using the Lattice Boltzmann method, *Int. J. Heat Mass Transfer*, vol. 49, n.3-4, pp. 727-739.

Fletcher, C.A.J. (1991): *Computational Techniques for Fluid Dynamics*, Springer-Verlag.

Gelfgat, A. Y (2006): Implementation of arbitrary inner product in the global Galerkin method for incompressible Navier-Stokes equations, *J. Comput. Physics*, vol. 211, pp. 513-530.

Guj, G.; Stella, F. (1993): A Vorticity-Velocity method for the Numerical Solution of 3D Incompressible Flows, *J. Comput. Physics*, vol. 106, n.2, pp. 286-298.

Labonia, G.; Stella, F.; Leonardi, E.; Guj, G. (1997): A numerical study of the effect of free surface deformation on buoyancy and thermocapillary convection, *J. Comput. Physics*, vol. 132, n.1, pp. 34-50.

Le Queré, P. (1991): Accurate solutions to the square thermally driven cavity at high Rayleigh number, *Computers & Fluids*, vol. 20, pp. 29-41.

Le Queré, P.; Behnia, M. (1998): From onset of unsteadiness to chaos in a differentially heated square cavity, *J. Fluid Mechanics*, vol. 359, pp. 81-107.

Lowrie, R.B. (2004): A comparison of implicit time integration methods for non-linear relaxation and diffusion, *J. Comput. Physics*, vol. 196, pp. 566-590.

Mansutti, D.; Bucchignani, E. (2005): Effects of solid deformations in the Gau & Viskanta gallium melting experiments, *Proc. 17th IMACS World Congress*, Paris (France) July, 2005.

Mayne, D.A.; Usmani, A.S.; Crapper, M. (2000): h-Adaptive finite element solutions of high Rayleigh number thermally driven cavity problem, *Int. J. Numer. Meth. Heat Fluid Flow*, vol. 10, pp. 598-615.

Ravi, M.R.; Henkes R.A.W.M.; Hoogendoorn C.J. (1994): On the high-Rayleigh-number structure of steady laminar natural-convection flow in a square enclosure, *J. Fluid Mechanics*, vol. 262, pp. 325-351.

Stella, F.; Guj, G.; Leonardi, E. (1993): The Rayleigh-Benard problem in intermediate bounded domains, *J. Fluid Mechanics*, vol. 254, pp. 375-400.

Stella, F.; Bucchignani, E. (1996): True transient vorticity-velocity method using

preconditioned Bi-CGSTAB, *Numerical heat transfer Part B*, vol. 30, pp. 315-339.

Stella, F.; Bucchignani, E. (1999): Rayleigh - Bénard convection in limited domains: Part 1 - Oscillatory flow, *Num. Heat Transfer Part A*, vol. 36, pp. 1-16.

Van der Vorst, H. (1992): Bi-CGSTAB, a fast and smoothly converging variant of Bi-CG for the solution of nonsymmetric linear systems, *SIAM J. Sci. Stat. Computing*, vol. 13, n.2, pp. 631-644.

Wan, D.C.; Patnaik, B.S.; Wei, G.W. (2001): A new benchmark quality solution for the buoyancy-driven cavity by discrete singular convolution, *Numerical Heat transfer Part B*, vol. 40, pp. 199-228.

